

LETTER

Multipath Fading Simulator Based on Distributed Scattering Model

Hidenori OKUNI[†], Student Member, Eisuke KUDOH[†], and Fumiyuki ADACHI[†], Members

SUMMARY Transmission performance of a multi-input multi-output (MIMO) antenna system (i.e., antenna diversity, adaptive antenna array, and space division multiplexing) highly depends on the arrival angle distribution of propagation paths. In this letter, a multipath fading simulator based on distributed scattering model is presented. The impacts of the arrival angle distribution of propagation paths on the bit error rates (BER) performance are measured using an implemented fading simulator and compared with the theoretically predicted performance.

key words: fading simulator, arrival angle distribution

1. Introduction

Recently, multi-input multi-output (MIMO) antenna system, i.e. antenna diversity [1], adaptive antenna array [2], and space division multiplexing [3] is attracting much attention in wireless communication systems. The mobile radio channel can be modeled as a multipath channel consisting of many paths having different time delays; the delay time spacing is the inverse of the signal bandwidth. Each path may be a cluster of many irresolvable paths having different Doppler shifts and different arrival angles. Furthermore, the nominal arrival angle and angle spread of each cluster of irresolvable paths change according to the movement of either a transmitter or a receiver. The transmission performance of a MIMO antenna system is highly affected by the arrival angle distribution of propagation paths, which depends on the locations of transmitter and receiver and the distribution of scatterers. Therefore, the fading simulator that can simulate various fadings with different values of arrival angle distribution is desirable to assess the transmission performance of various MIMO antenna systems. In Ref. [4], a structure of fading simulator is presented which can control the arrival angle spread of each of the irresolvable paths by multiplying a nominal path by the antenna steering vector. Using this method, all generated irresolvable paths in a cluster have the same Doppler shift. However, this is not the case in the real environment.

In this letter, we present a fading simulator that can control the arrival angle distribution of the irresolvable paths based on the distributed scattering model. Using this model, a cluster of irresolvable paths having different Doppler shifts and arrival angles can be generated according to the location and traveling speed of a mobile terminal. In Sect. 2,

the distributed scattering model is introduced and a fading simulator based on this model is presented. In Sect. 3, the impacts of nominal arrival angle and arrival angle spread of irresolvable paths on the bit error rate (BER) performance are measured using the implemented fading simulator and compared with the theoretically predicted performance to confirm that the implemented simulator works as designed.

2. Fading Simulator

There are several scattering models, e.g., ring model [1], limited arrival angle model [4], distributed scattering model [5], etc. In this letter, we use a distributed scattering model, in which N scattering obstacles are randomly located inside a circle with a radius r around the transmitter as shown in Fig. 1. We consider M -branch antenna receive diversity, where the antennas are linearly placed with a separation d . The received signal $z_m(t)$ at the m ($=0 \sim M-1$)-th antenna can be expressed using the equivalent base-band representation as

$$z_m(t) = \sum_{l=0}^{L-1} \xi_{m,l}(t) s(t - \tau_l), \quad (1)$$

where $s(t)$ is the transmit signal, L is the number of resolvable paths, $\xi_{m,l}(t)$ is the complex path gain of the l -th resolvable path associated with the m -th antenna, and τ_l is the delay time of the l -th resolvable path. Each resolvable path is a cluster of N irresolvable paths with the same delay time. $\xi_{m,l}(t)$ is expressed as

$$\xi_{m,l}(t) = \sum_{n=0}^{N-1} \xi_{m,l,n}(t), \quad (2)$$

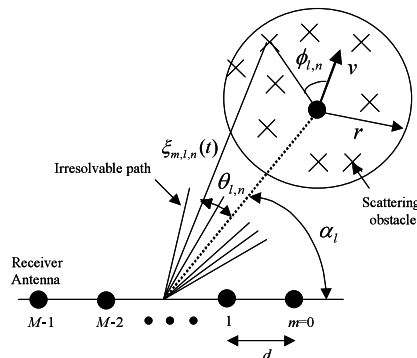


Fig. 1 Distributed scattering model.

Manuscript received February 9, 2004.

Manuscript revised March 26, 2004.

[†]The authors are with the Dept. of Electrical and Communication Engineering, Graduate School of Engineering, Tohoku University, Sendai-shi, 980-8579 Japan.

where $\xi_{m,l,n}(t)$ is the complex path gain of the n -th irresolvable path. In Fig. 1, the n -th irresolvable path that consists of the l -th resolvable path arrives from the angle of $\alpha_l + \theta_{l,n}$, where α_l is the nominal arrival angle of the l -th resolvable path. $\phi_{l,n}$ is the angle between the traveling direction of the transmitter and the scattering obstacle which generates the n -th irresolvable path. $\xi_{m,l,n}(t)$ is given by

$$\xi_{m,l,n}(t) = A_{l,n} \exp j \left[2\pi \left\{ \frac{f_D t \cos \phi_{l,n}}{+ \frac{d}{\lambda} \left(\frac{M-1}{2} - m \right) \cos(\alpha_l + \theta_{l,n})} \right\} + \psi_{l,n} \right], \quad (3)$$

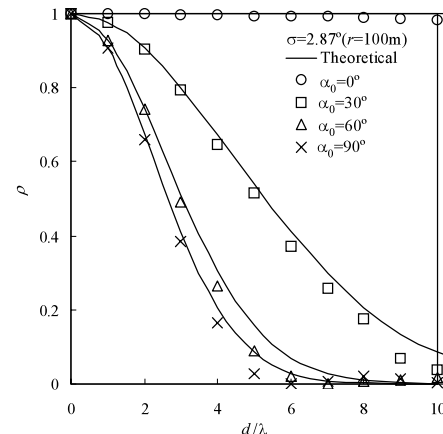
where $f_D (=v/\lambda)$ is the maximum Doppler frequency, v is the traveling speed of the transmitter and λ is the carrier wavelength. $A_{l,n}$ and $\Psi_{l,n}$ are the amplitude and the phase of the n -th irresolvable path, respectively.

The impact of the nominal arrival angle α_0 and the angle spread σ on the fading envelope correlation ρ between $|\xi_{0,l}(t)|$ and $|\xi_{1,l}(t)|$ is discussed below. It is assumed that the transmitter is located at a distance of 1000 m from the receiver ($R=1000$ m) and 32 scattering obstacles ($N=32$) are randomly located inside the circle with a radius $r=10\sim 300$ m. It is also assumed that each irresolvable path has equal amplitude $A_{l,n} = 1/\sqrt{N}$ and uniformly distributed phase $\Psi_{l,n}$ over $[0, 2\pi]$. Thus, the arrival angle spread $\sigma \left(= \sqrt{(1/N) \sum_{n=0}^{N-1} \theta_{l,n}^2} \right)$ becomes $\sigma=0.287\sim 8.60^\circ$ for $r=10\sim 300$ m. Figures 2(a) and (b) plot ρ as a function of the antenna separation d with the arrival angle α_0 and the angle spread σ as parameters, respectively. Also plotted for comparison in Fig. 2 is the theoretically predicted curve [5]:

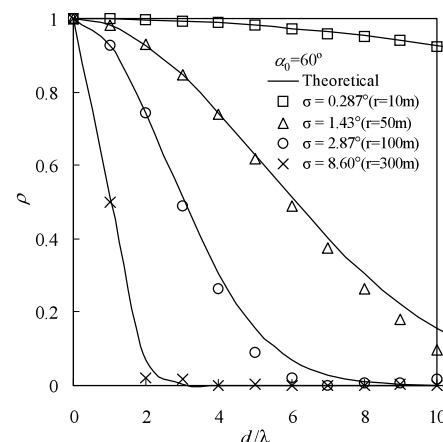
$$\rho \approx \exp \left[- \{ 2\pi\sigma(d/\lambda) \sin(\alpha_l) \}^2 \right]. \quad (4)$$

As seen from Fig. 2, the fading envelope correlation is significantly affected by the nominal arrival angle and the angle spread.

The distributed scattering model-based fading simulator can generate fading with different values of nominal arrival angle and angle spread according to the transmitter and receiver locations and scatterers' distribution. The distributed scattering model-based fading simulator generates $\xi_{m,l}(t)$ using Eq. (2) and then produces the faded signal using Eq. (1). Figure 3 illustrates the block diagram of an implemented fading simulator for the case of $L = M=2$. The transmitted signal $s(t)$ at a carrier frequency of 240.1 MHz is down-converted to the in-phase (I) and quadrature-phase (Q) signals which are sampled by a 12-bit analog-to-digital (A/D) converter. In a field programmable gate array (FPGA), delayed versions of the I and Q signals are produced and each signal is multiplied by the complex fading envelope $\xi_{m,l}(t)$ which is generated using Eq. (2) by a digital signal processor (DSP). The faded signals from the FPGA are converted to analog faded signals by 12-bit digital-to-analog (D/A) converter and then up-converted to RF fading signals.



(a) Impact of nominal arrival angle.



(b) Impact of angle spread.

Fig. 2 Fading envelope correlation for $R=1000$ m.

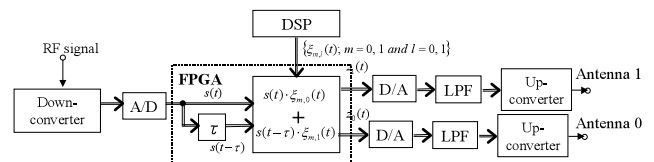


Fig. 3 Block diagram of fading simulator for $L = M=2$ case.

3. Transmission Performance Measurement Using Implemented Fading Simulator

Figure 4 illustrates the block diagram of an experimental system with a radio carrier frequency of 240.1 MHz. Table 1 summarizes the experimental condition. Binary phase shift keying (BPSK) data modulation is used. The frame structure of the transmitted signal is illustrated in Fig. 5. A frame consists of 60 BPSK data symbols and 4 pilot symbols. In the receiver, 2-antenna ($M=2$) maximal ratio combining (MRC) diversity is used and channel estimation for coherent detection is carried out by simple averaging of 4 received pilot symbols.

The measured BER performance for the case of $L=1$ is shown in Fig. 6. Figure 6(a) shows the impact of the nom-

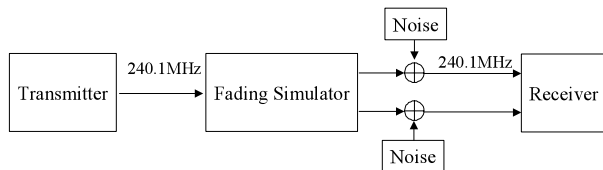


Fig. 4 Block diagram of experimental system.

Table 1 Experimental condition.

Transmitter parameter	Modulation	BPSK
	Transmit/receive filter	Root roll off filter (roll off factor=0.5)
	Data rate	31.67kbps
	Frame structure	Pilot:4symbols Data:60symbols
	Carrier frequency	240.1MHz
Propagation model	No. of resolvable paths	$L=1, 2$
	No. of irresolvable paths	$N=32$
	Maximum Doppler frequency	$f_D=5\text{Hz}$
Antenna diversity combining		2-branch MRC

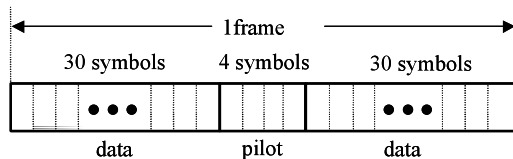
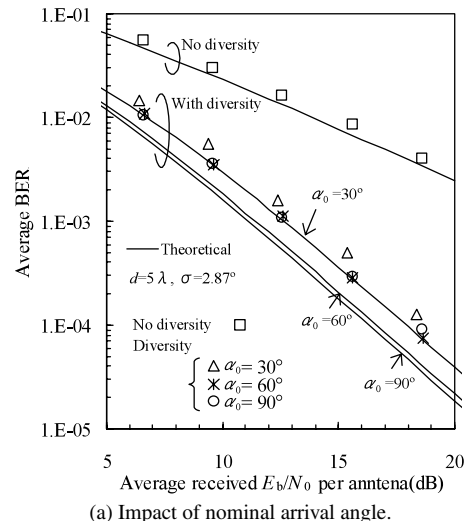


Fig. 5 Frame structure.

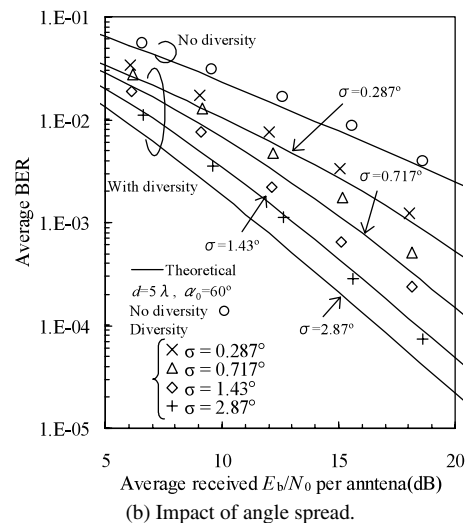
inal arrival angle α_0 for $L=1$, $\sigma = 2.87^\circ$ (this corresponds to $R=1000$ m and $r=100$ m) and $d=5\lambda$. Figure 6(b) shows the impact of the arrival angle spread σ ($r=10\sim 100$ m for $R=1000$ m) for $L=1$, $\alpha_0=60^\circ$ and $d=5\lambda$. For comparison, the theoretical BER performance is also plotted. The theoretical BER with 2-antenna MRC diversity is given by (see Appendix A)

$$P_b(\Gamma) = \frac{1}{2} + \frac{1}{4\sqrt{\rho}} \left\{ \begin{array}{l} \frac{1 - \sqrt{\rho}}{\sqrt{1 + \frac{1}{(1 - \sqrt{\rho})\Gamma}}} \\ 1 + \sqrt{\rho} \\ - \frac{1 - \sqrt{\rho}}{\sqrt{1 + \frac{1}{(1 + \sqrt{\rho})\Gamma}}} \end{array} \right\}, \quad (5)$$

where Γ is the average received signal energy per bit-to-noise power spectrum density ratio E_b/N_0 per antenna and the fading envelope correlation ρ is given by Eq. (4). As α_0 or σ becomes smaller, ρ becomes larger and hence, the BER performance degrades due to the reduction in diversity effect. The measured BER performance close to the theoretical one is obtained. An E_b/N_0 degradation of about 1.5 dB is due to the pilot insertion loss (0.28 dB) and the channel



(a) Impact of nominal arrival angle.



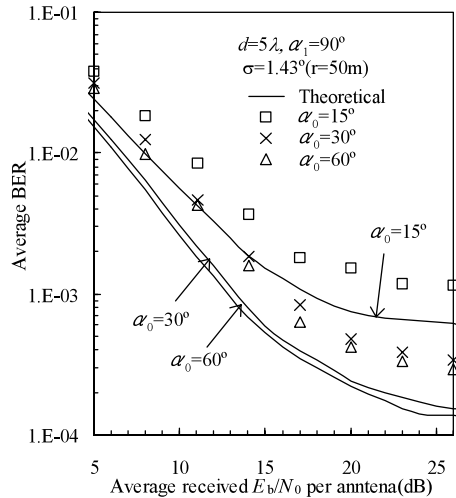
(b) Impact of angle spread.

Fig. 6 BER performance for $L=1$, $R=1000$ m, and $M=2$.

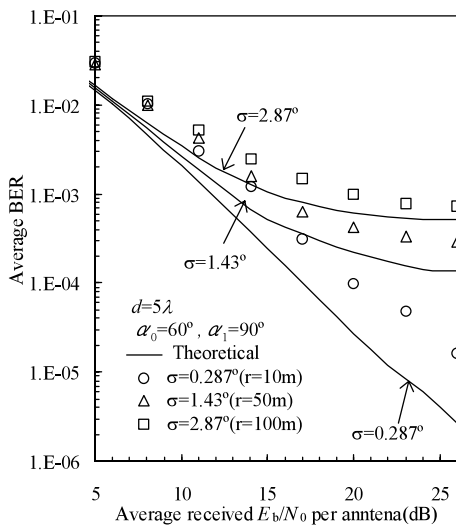
estimation error (0.97 dB) [6].

The measured BER performance for the case of two-path channel ($L=2$) of equal average power is shown in Fig. 7. Figure 7(a) shows the impact of the nominal arrival angle α_0 for $L=2$, $\Delta\tau/T = (\tau_1 - \tau_0)/T = 0.34$, $\sigma=2.87^\circ$ and $d=5\lambda$. Figure 7(b) shows the impact of the arrival angle spread σ for $L=2$, $\Delta\tau/T = 0.34$, $\alpha_0=60^\circ$ and $d=5\lambda$. For comparison, the theoretical BER performance curve is also plotted (see Appendix B). The BER performance degrades due to increasing inter-symbol interference (ISI) and hence BER floors are produced for large E_b/N_0 . As α_0 decreases or σ increases, the fading envelope correlation ρ becomes larger and hence the BER floor increases due to the decrease in the diversity effect.

As understood from Figs. 6 and 7, the BER performance of antenna diversity system is affected by the nominal arrival angle and angle spread of the irresolvable paths (i.e., arrival angle distribution). This is also true for adaptive antenna array and space division multiplexing. Since the distributed scattering Δ -based fading simulator can



(a) Impact of nominal arrival angle.



(b) Impact of angle spread.

Fig. 7 BER performance for $L=2$, $R=1000$ m, and $M=2$.

control the arrival angle distribution of irresolvable paths, it can be used for assessing the transmission performance of MIMO antenna systems.

4. Conclusions

A distributed scattering model-based fading simulator was presented that can generate various fading with different arrival angle distribution of the propagation paths according to the transmitter location and the scatterers' distribution and hence can be used to assess the performance of various MIMO antenna systems. The fading simulator was implemented and the BER performance of 2-antenna diversity system measured to show the impact of the nominal arrival angle and arrival angle spread on the BER performance. The measured BER performance was compared with the theoretical one to confirm that the implemented simulator works as designed.

References

- [1] W.C. Jakes, Jr., Microwave mobile communications, John Wiley, New York, 1974.
- [2] R.T. Compton, Adaptive antennas, Prentice Hall, Engle Wood Cliffs, 1988.
- [3] G.J. Foshini and M.J. Gans, "On limits of wireless communications in a fading environment when using multiple antennas," Wireless Pers. Commun., vol.6, no.3, pp.311-355, March 1998.
- [4] T. Poutanen and J. Kolu, "Correlation control in the multichannel fading simulators," Proc. IEEE VTC, Rhodes, pp.318-322, May 2001.
- [5] F. Adachi, M.T. Feeney, A.G. Williamson, and J.D. Parsons, "Cross-correlation between the envelopes of 900 MHz signals received at a mobile radio base station site," IEE Proc., Pt. F, vol.133, no.6, pp.506-516, Oct. 1986.
- [6] S. Takaoka and F. Adachi, "Pilot-aided adaptive prediction channel estimation in a frequency-nonselctive fading channel," IEICE Trans. Commun., vol.E85-B, no.8, pp.1552-1560, Aug. 2002.
- [7] M. Schwartz, W.R. Bennett, and S. Stein, Communication systems and techniques, McGraw-Hill, 1966.

Appendix A: Theoretical BER with 2-Antenna MRC Diversity when $L = 1$

For 2-antenna MRC diversity, the probability density function (pdf) $p(\gamma)$ of the instantaneous received E_b/N_0 γ is given by [7]

$$p(\gamma) = \frac{1}{\lambda_1 - \lambda_2} \left\{ \exp\left(-\frac{\gamma}{\lambda_1}\right) - \exp\left(-\frac{\gamma}{\lambda_2}\right) \right\} \quad (A.1)$$

where

$$\lambda_1 = (1 + \sqrt{\rho})\Gamma, \quad \lambda_2 = (1 - \sqrt{\rho})\Gamma. \quad (A.2)$$

The average BER $P_b(\Gamma)$ is given by

$$P_b(\Gamma) = \int_0^\infty \frac{1}{2} \operatorname{erfc} \sqrt{\gamma} \cdot p(\gamma) d\gamma$$

$$= \frac{1}{2} + \frac{1}{4\sqrt{\rho}} \left\{ \frac{\frac{1 - \sqrt{\rho}}{\sqrt{1 + \frac{1}{(1 - \sqrt{\rho})\Gamma}}}}{1 + \sqrt{\rho}}}{\sqrt{1 + \frac{1}{(1 + \sqrt{\rho})\Gamma}}} \right\}. \quad (A.3)$$

Appendix B: Theoretical BER with 2-Antenna MRC Diversity when $L = 2$

The receiver sampling timing is locked to the middle point between the first and second paths. The inter-symbol interference (ISI) produced due to delayed path is approximated as a Gaussian noise. For the given $\{\xi_{m,l}; m=0,1 \text{ and } l=0,1\}$, the instantaneous received signal-to-ISI plus noise power ratio (SINR) after 2-antenna MRC diversity is given by

SINR

$$\begin{aligned}
 &= \frac{2\Gamma \sum_{m=0}^1 \left| \xi_{m,0}h(\Delta\tau/2) + \xi_{m,1}h(-\Delta\tau/2) \right|^2}{1 + \Gamma \sum_{\substack{n=-\infty \\ n \neq 0}}^{+\infty} \left| \sum_{m=0}^1 \left[\begin{aligned} &\{\xi_{m,0}h(-nT + \Delta\tau/2) + \xi_{m,1}h(-nT \\ &- \Delta\tau/2)\} \times \{\xi_{m,0}h(\Delta\tau/2) \\ &+ \xi_{m,1}h(-\Delta\tau/2)\}^* \end{aligned} \right] \right|^2}, \\
 &\qquad \sum_{m=0}^1 \left| \xi_{m,0}h(\Delta\tau/2) + \xi_{m,1}h(-\Delta\tau/2) \right|^2
 \end{aligned} \tag{A.4}$$

where $h(t)$ is the impulse response of overall trans-

mit/receive filter, Γ is the average E_b/N_0 , $\Delta\tau$ ($= \tau_1 - \tau_0$) is the delay time difference between 2 paths, T is the BPSK symbol period. The conditional BER $P_b(\{\xi_{m,l}\})$ is given by

$$P_b(\{\xi_{m,l}\}) = \frac{1}{2} \operatorname{erfc} \sqrt{\frac{SINR}{2}}. \tag{A.5}$$

The average BER $P_b(\Gamma)$ can be numerically evaluated by generating a set of $\{\xi_{m,l}\}$ based on the distributed scattering model, computing the conditional BER using Eq. (A.5) and repeating the process a number of times.